Composites Part B 160 (2019) 446–456

Contents lists available at ScienceDirect

Composites Part B

journal homepage: www.elsevier.com/locate/compositesb

The influence of surface treatment on the tensile properties of carbon fiber-reinforced epoxy composites-bonded joints

Guanxia Yang, Tao Yang*, Wenhui Yuan, Yu Du

School of Mechanical Engineering, Tianjin Polytechnic University, Tianjin, 300387, China

ARTICLE INFO

Keywords:
Composite-bonded joints
Surface treatment
Tensile properties
Surface characterization

ABSTRACT

The surface characteristics of carbon fiber-reinforced composites significantly influence the tensile properties of adhesive-bonded joints. The main objective of this study was to research the effect of surface treatment by sandpaper rubbing on the strength of adhesive joints. In the present research, surfaces were prepared using four grades of sandpaper with grit sizes of up to 60, 220, 400, 800, and polish grit. Further, the two types of joints (single lap joint and scarf adhesive joint) were tested to investigate the effects of the grit sizes and sanding direction of the sandpaper (parallel to the fiber direction, perpendicular to the fiber direction, and random direction) on the tensile properties. The experimental results showed that the highest bonding strength could be achieved when the surface was sanded in the random direction. Moreover, the grit sizes of the sandpaper significantly influenced the surface characteristics, including the surface profile, surface roughness, surface contact angle, and surface free energy of the specimens, and then affected the bonding strength of the joints by mechanical interlocking and adsorption effect. Furthermore, for both single lap and scarf adhesive joints, the failure mode and the force of the adhesive layer under tensile load were different; therefore, the dominant factors affecting the bonding enhancement mechanism were consequently different.

1. Introduction

Composite structures are inevitably subjected to a variety of defects introduced during manufacturing and service. In order to ensure normal operation of the original system, these damaged structures need to be restored through component replacement or certified repair [1–3]. For these large integrated components; however, it is infeasible to achieve structural replacement due to high cost and long period of service. Therefore, composite repair technologies have received significant attention with the objective of restoring structural efficacy by repair [4–6]. Moreover, many repair strategies are increasingly using adhesive-bonded joints as alternatives to traditional mechanical fasteners because of their great advantages such as cost effectiveness, small stress concentration, excellent structural integrity, and simple operation. However, adhesive joints are usually the weakest part of a structure due to the discontinuity of reinforcing fibers at the joint interfaces [7,8]. Therefore, it is extremely important to enhance the bonding strength to improve the life and durability of the product [9]. The main objective of this study was to enhance the bonding strength of carbon fiber-reinforced plastic (CFRP) composites joints by surface treatment using sandpaper and research the influence of surface treatment on the tensile properties of these joints.

An adhesive-bonded joint is composed of three parts, namely, the substrate, adhesive layer, and interfaces between substrates and adhesive. For specific substrate and adhesive, it is critical to boost the interface to improve the bonding strength of the joints [10–12]. Furthermore, the interface between the substrate and adhesive is extensively associated with the surface characteristics such as the surface free energy, surface topography, and roughness of the substrate. The surface free energy of a material is an important parameter of its surface characteristics, and has a significant role in the adhesion, adsorption, and wettability of material [13]. In general, the good wettability and adhesion properties can be achieved when the surface energy of a solid is higher than that of a liquid [14]. Moreover, according to the adsorption theory, the higher the surface free energy, the stronger the adhesion force, which indicates greater bonding force with other materials. Therefore, many researchers focused on the study of improving the bonding strength by increasing the surface energy of the substrates [15,16]. Furthermore, several methods are available to calculate the surface free energy by measuring the contact angles of liquids. These methods include Fowkes, Owens–Wendt, Van Oss–Chaudhury–Good, Fox–Zisman, and Neumann methods. Each method has its own advantages and application prospects [17,18]. For the CFRP substrate, the Owens–Wendt method has been adopted by many researchers [10,19].

* Corresponding author.
E-mail address: yangtao@tjpu.edu.cn (T. Yang).

https://doi.org/10.1016/j.compositesb.2018.12.095
Received 19 July 2018; Received in revised form 4 December 2018; Accepted 17 December 2018
Available online 19 December 2018
1359-8368/

Moreover, the surface morphology and roughness directly affect the flow and spread of the adhesive on the substrate surface. Proper surface roughness may promote the penetration of adhesive into the substrate, and subsequently enhance the specific area of the bonding region [12,20]. Furthermore, the mechanical interlocking theory describes that after the adhesive fills the gap of the substrate surface, the cured adhesive forms meshing connections with the irregular topography of the substrate surface [12]. Moreover, it was also found that the effect of mechanical interlocking enhanced with the surface roughness, and subsequently improved the bonding strength [21]. Gude et al. [10] investigated the correlation between surface characteristics (roughness and surface free energy) and mechanical properties of the adhesive joints. Experimental results indicated that mechanical interlocking was the main adhesion mechanism for the mode I testing, whereas the shear strength did not increase with a rougher surface, and the polar component of the surface free energy exhibited a more significant effect on shear strength. Islam et al. [13] studied several different performance of glass fiber-reinforced polymer coating, and found that the dolly pull-off strength improved with the increase in the surface roughness of the substrate within a certain scope. Once beyond the scope, the dolly pull-off strength was found to be reduced.

Noteworthy, surface characteristics are directly related to the surface treatment. For neutral substrate, surface treatment is an effective method to generate dipoles on the substrate and increase the surface energy and wettability as well [12,22,23]. Therefore, extensive research efforts have been devoted to the investigation of different surface treatments including solvent cleaning [24], infrared- and ultraviolet-laser pretreatment [23,25,26], abrasion, peel-ply [10,24,27], acid chemical etching [27,28], and plasma treatments [10,27,29] to improve the surface characteristics, and further enhance the bonding strength. Chemical process such as plasma treatment aims to functionalize the substrate to increase the surface energy, and thus promotes adhesion by providing specific interactions across the adhesive–adherend interfaces [24]. Solvent wipe or abrasion is a typical physical method of surface treatment, which aids in removing contaminants and producing a rough surface. By using abrasion and cleaning steps, an increase in roughness and bond strength has been observed for steel epoxy/glass composites-bonded joints [22].

Mechanical treatment of surface with sandpaper is a simple and practical method to achieve desired surface characteristics. This treatment can produce different surface roughness based on the sandpaper mesh numbers, and the sanding direction can also be controlled to produce the required surface texture as well. Many researchers have examined the effect of surface characteristics such as surface roughness and surface free energy acquired by different treatment methods on the strength and durability of adhesive joints using various adherends and adhesives. However, specialized research about the effect of sanding preparation including the grit size and the direction of sanding on the bonding performance of CFRP joints has rarely been reported till date. Boutar et al. [30] studied the effect of surface roughness and wettability on the strength of aluminum single lap joints, and reported that the smaller the surface roughness, the better the bonding performance. However, carbon fiber laminates are anisotropic materials which are different from aluminum; therefore, results from literature reports can be used as reference, but cannot be completely applied to the laminated composites. As a result, it is necessary to further study the effect of surface characteristics on CFRP composites adhesive joints, in particular, the surface characteristics by sanding preparation.

In this study, first, three sanding directions (parallel to the fiber direction, perpendicular to the fiber direction, and random direction) were studied briefly to investigate their effect on the tensile strength of the singe lap joints. Further, surfaces were prepared using four grades of sandpaper with grit sizes up to 60, 220, 400, and 800 and polish processing to study the influence of roughness of the sandpaper on the tensile properties for two types of joints (single lap and scarf adhesive joints were fabricated and tested). Finally, the surface parameters including the surface profile, surface roughness, surface contact angle, and surface free energy of the specimens before being bonded were measured to study the influence mechanism of surface treatment on the tensile properties of the bonded joints.

2. Experiments

2.1. Materials and surface treatment

Carbon fiber composite substrates were fabricated from 12 plies of T300 carbon-fiber/epoxy-prepreg with the stacking sequence of $[0/90]_{3S}$. The fiber density of prepreg was 1.77 g/cm^3 and the thickness of each layer was 0.15 mm. The substrates, with dimensions of 300 mm × 250 mm × 1.8 mm, were cured and consolidated in an autoclave at 80 °C for 1 h, and then at 120 °C for 1.5 h in accordance with the manufacturer's recommended cure process. Then the laminates were cut to ensure the final dimension of the specimens to be 250 mm × 25 mm × 1.8 mm. A two-component epoxy adhesive Araldite 2015 was used to bond the joints in a mixing ratio of 1:1 by volume.

A single factor experiment was carried out employing the following three variables: the sanding direction, the grit size of the sandpaper, and the joint types. The specific surface treatment methods and sample grouping are summarized in Table 1, and five samples were tested for each group. For the single lap joints, the substrate surfaces were sanded directly using sandpapers with different grit sizes up to 60, 220, 400, and 800 and polish to eliminate the resin and dirt present on its surface. For the scarf adhesive joints, the substrates were ground using a pre-grinding machine to remove a large amount of the inclined surface materials, and then the inclined surface was sanded using sandpapers with different grit sizes of 60, 220, 400, and 800 and polish until predetermined scarf angles were obtained. After grinding, substrates were washed under tap water, degreased with acetone for 10 min, and finally cleaned with distilled water to achieve a good bonding surface.

2.2. Measurements of surface characteristics

The macroscopic surface topography and the three-dimensional (3D) microscopic surface topography of the samples were obtained using a Leica microscope (Leica DVM6) and white confocal microscope (Zeiss CSM700), respectively. The analysis area of the 3D microscopic surface topography was 30 μm × 30 μm. Furthermore, the surface roughness was also measured using a white confocal microscope (Zeiss CSM700). When measuring the surface roughness, five points with the measurement area of 130 μm × 130 μm were selected for each sample, and the distribution of each point is shown in Fig. 1. Finally, the average values of the surface roughness of all the measurement areas in

Table 1
Surface treatment and sample grouping.

Groups	Joint types	Paper mesh number	Sanding direction
A1	Single lap	220	Parallel to the fiber
A2	Single lap	220	Perpendicular to the fiber
A3	Single lap	220	Random direction
B1	Single lap	60	Random direction
B2	Single lap	220	Random direction
B3	Single lap	400	Random direction
B4	Single lap	800	Random direction
B5	Single lap	Polish	Random direction
C1	Scarf	60	Random direction
C2	Scarf	220	Random direction
C3	Scarf	400	Random direction
C4	Scarf	800	Random direction
C5	Scarf	polish	Random direction

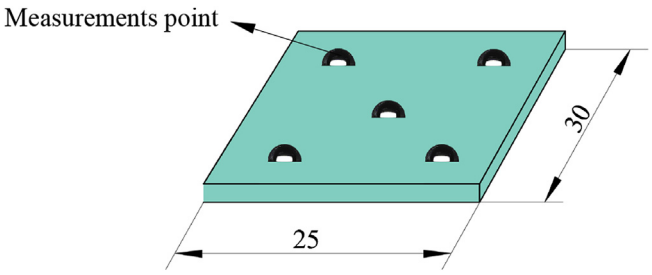

Fig. 1. Measurement point distribution on the bonding surface (dimensions in mm).

each group were considered as the average surface roughness.

The static surface contact angles of the various samples were measured using a contact angle analyzer (Krüss DSA30). A digital camera located on the analyzer was used to capture the pictures of the drops, and the JC2000DB software was used to analyze these pictures. To calculate the surface energy by Owens–Wendt method (Eq. (1)), two liquids, i.e. distilled water as a polar liquid and diiodomethane as a non-polar liquid, were selected to measure the contact angle. Five measurement points were selected for each sample, and three samples were tested for each group, that is 15 measurements were made for each group. The measurement point distribution is shown in Fig. 1. The data were achieved from the average values of the 15 measurements of each group. Moreover, combined with the surface tension balance equation of the solid–liquid–gas triple point (Eq. (2)), the surface free energy σ_s with its polar component σ_s^p and dispersive component σ_s^D of the specimens were also calculated [31] as follows:

$$\gamma_{sl} = \sigma_s + \sigma_l - 2(\sqrt{\sigma_s^D \times \sigma_l^D} + \sqrt{\sigma_s^P \times \sigma_l^P}) \quad (1)$$

$$\sigma_s = \gamma_{sl} + \sigma_l \times \cos(\theta) \quad (2)$$

where θ is the contact angle, and γ_s^l is surface tension of solid–liquid phase interface, and σ_s and σ_1 correspond to the surface free energy of the substrate and the surface tension of the liquid (distilled water and diiodomethane), respectively. The superscripts D and P represent the dispersive and polar fractions, respectively, and the total surface energy is the sum of both fractions.

2.3. Fabrication of joints and tensile test

The substrates were bonded after surface treatment, and then cured at room temperature under a constant pressure of 0.12 MPa for 48 h. For the single lap joints, the two ends were not in the same plane; therefore, two aluminum plates with the same thickness as the substrate were pasted on both ends of the joint to avoid the deviation of the action line during the test. Fig. 2 shows the geometry and dimensions of the two types of samples.

Fig. 3 exhibits that the tensile test platform was a computer controlled testing machine (Shimadzu AGS-X). The unidirectional tensile test method was adopted under 2 mm/min loading speed according to the ASTM D3039 [32] standard. During the test, the load and displacement of the test samples in real time were recorded using the commercial general software Tropezium Lite. Finally, the experimental data were analyzed to obtain the maximum load and tensile strength of each group, and further the failure morphology was examined.

3. Results and discussion

3.1. Tensile strength

The load versus displacement curves are the most intuitive basis to study the mechanical performance of adhesive joints. Fig. 4 shows the typical load versus displacement curves of single lap joint and scarf adhesive joint abraded using sandpaper with grit sizes of 60, 220, 400, 800, and polished finish. Clearly, the tensile load suddenly drops when it reaches the maximum value, and the specimens undergo sudden failure.

Table 2 lists the average maximum tensile load and standard deviation of each group. Clearly, the maximum tensile load of the samples in the same group fluctuates slightly. In order to incorporate the effect of the deviation of experimental data obtained from possible random errors in the test process on the difference between the experimental groups, the One-Way analysis of variance (ANOVA) of the maximum tensile load was carried out, and the obtained results are listed in Table 3.

Table 3 summarizes that the grinding direction of the sandpaper significantly influences the bonding strength, and the confidence of the significant influence is 97.5%. Moreover, the roughness of the sandpaper has a great effect on the bonding strength as well, and the confidence of the significant influence for the single lap joint and the scarf adhesive joint is 99 and 97.5%, respectively. Therefore, the average maximum tensile load of each group could be used to evaluate the difference in bonding performance.

The tensile strength of the sample was calculated according to Eqs. (3) and (4), and the tensile and shear strength of each group were obtained, as shown in Fig. 5(a)–(c).

$$\tau = F_{MAX}/l{\cdot}w \quad (3)$$

$$\sigma = F_{MAX}/t{\cdot}w \quad (4)$$

where F_{MAX} is the maximum tensile load of the samples; τ is the shear strength of the single lap joint and σ is the tensile strength of the scarf adhesive joint; and $l = 30$ mm, $w = 25$ mm, and $t = 1.8$ mm are the bond length of the single lap joint, and the width and the thickness of the joint, respectively.

Fig. 5(a) shows that the direction of sanding significantly affects the tensile strength of the joint. When grinding was carried out in the random direction, the shear strength of the single lap joint was 17.58 MPa, which was 9.91 and 9.16% higher than that of unidirectional grinding (when parallel to the fiber direction, the shear strength was 16.00 MPa; and when perpendicular to the fiber direction, it was 16.11 MPa). This result might be attributed to the fact that when sandpaper was used perpendicular to the fiber direction, the surface fibers of the samples were easily cut off by the abrasive grain. When grinding was carried out parallel to the fiber direction, the surface fibers tended to form an isolated fiber bundle along the grinding direction. Furthermore, more broken short fibers were still attached to the surface of the samples due to the single grinding direction, which made the surface loose in texture and in turn influenced the bonding effect. However, for the random grinding of the sample, the surface was completely polished in various directions, and the loose fibers on the sample surface were removed sufficiently. Therefore, the corresponding bonding effect was better.

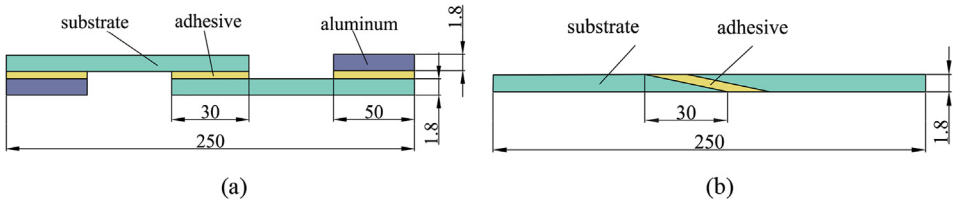

Fig. 2. Geometry and dimensions of (a) the single lap joint and (b) scarf adhesive joint (dimensions in mm).

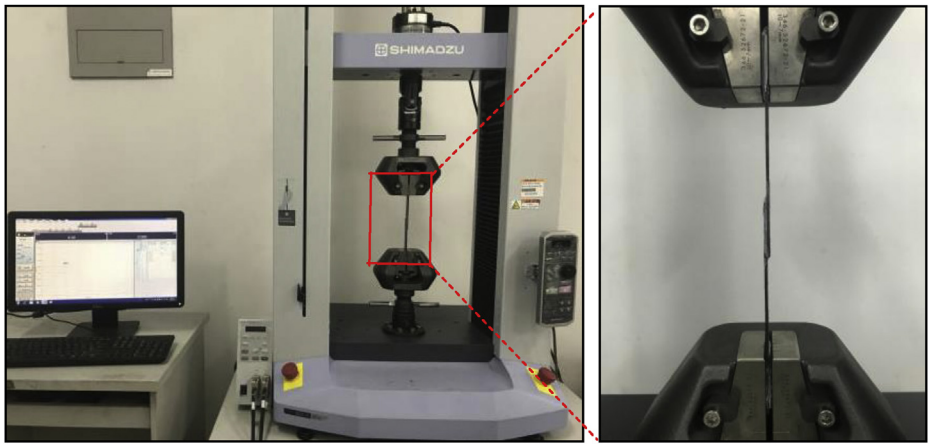

Fig. 3. Experimental setup of tensile test.

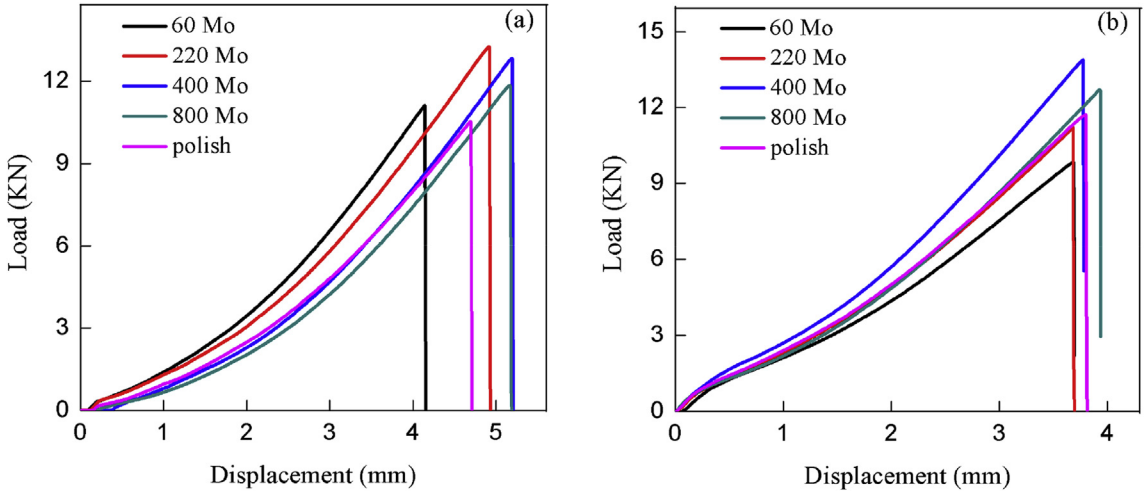

Fig. 4. The typical load versus displacement curves of (a) single lap joint and (b) scarf adhesive joint with 60, 220, 400, 800 grit sizes of sandpapers and polish prepared.

Table 2
Average maximun tensile load and standard deviation.

Groups	Average tensile load (N)	Standard deviation (N)
A1	12001.2	572.71
A2	12084.1	592.74
A3	13190.4	712.57
B1	11214.5	772.56
B2	13190.4	712.57
B3	12387.6	902.35
B4	12128.2	903.34
B5	10784.5	609.24
C1	11639.7	933.39
C2	11754.8	542.25
C3	12915.8	822.96
C4	12577.7	678.91
C5	11862.2	631.14

Table 3
Variance analysis.

Groups	Degrees of freedom	Intra-group variation	Inter-group variation	F	$F_{0.01}$	$F_{0.025}$
A	14	4748352	4407537	5.569	6.93	5.10
B	24	12386900	18340244	7.403	4.43	3.51
C	24	10788574	7625192	3.533	4.43	3.51

Fig. 5(b) and (c) demonstrate that the tensile strength appears to first increase and then decrease slightly for the specimens treated using sandpaper with grit size of 60 compared to those prepared using polish grit for both the single lap joint and scarf adhesive joint. For the single lap joint (Fig. 5(b)), the shear strength of samples abraded using sandpaper with grit sizes of 60, 220, 400, 800, and polished finish were 14.95, 17.58, 16.52, 16.17, and 14.38 MPa, respectively. An optimum shear strength value of 17.58 MPa was obtained for the surfaces abraded with 220 grit size, which increased by 17.62 and 22.31%, respectively, compared to the grit sizes of 60 and polishing process. Moreover, the bearing capacity of the joint was also the best as indicated by the values of standard deviation listed in Table 2. For the scarf adhesive joints (Fig. 5(c)), the tensile strengths of the specimens abraded using 60, 220, 400, 800 and polish grit sizes sandpaper were 258.66, 261.22, 287.02, 279.51, and 263.60 MPa, respectively. The best tensile strength was achieved when samples were abraded using sandpaper with 400 grit size, which exhibited an increase by 11.0% and 8.9%, respectively, compared to the sandpaper with grit sizes of 60 and polish processing.

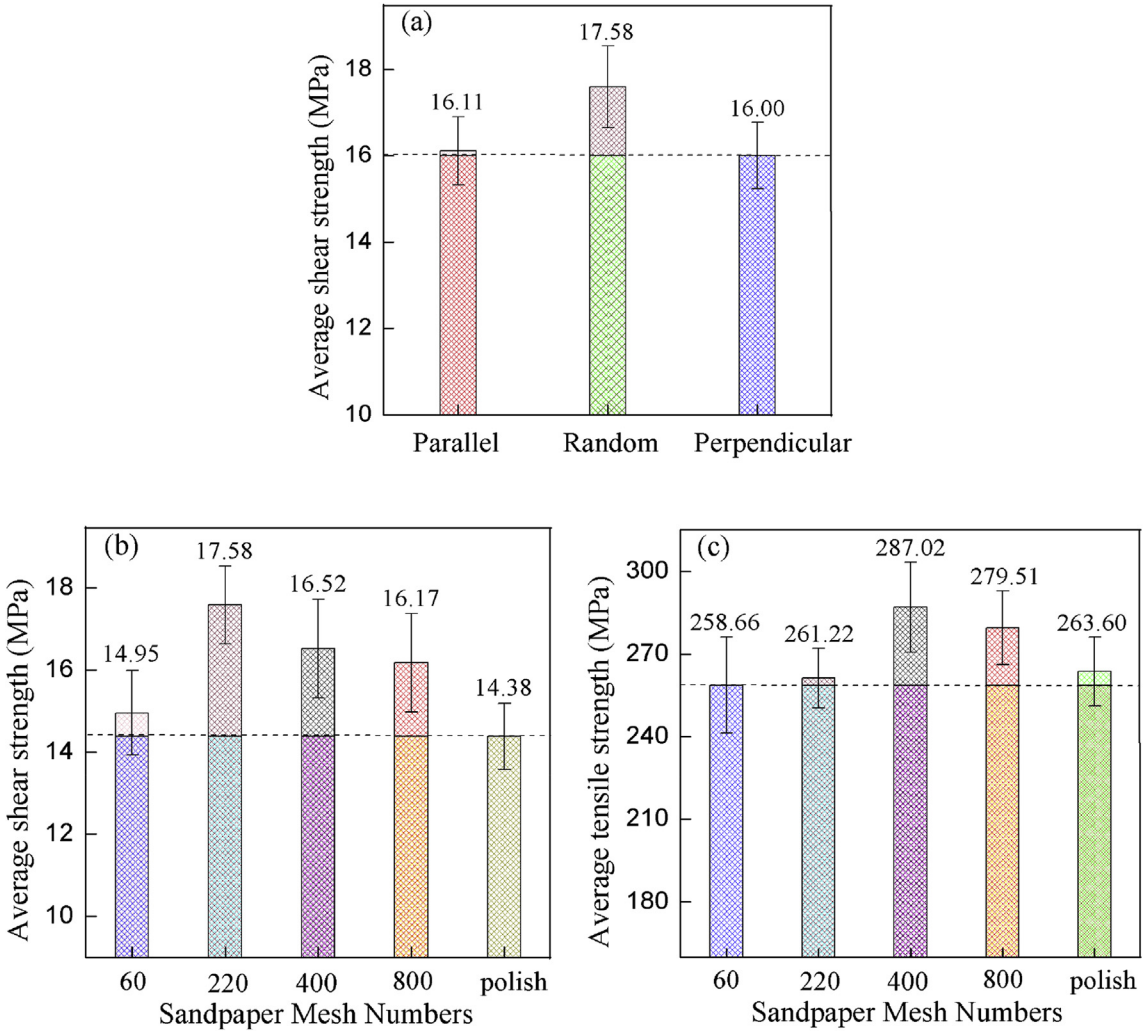

Fig. 5. The tensile strength of (a) Group A, (b) Group B and (c) Group C.

3.2. Surface characterization

3.2.1. Surface topography and surface roughness

Figs. 6 and 7 show the macroscopic topography, local magnification, and 3D microscopic topography of the bonding surface. The scratch on the bonding surface appears to be shallower, and the surface becomes smoother at a macro level for the specimens from sanded with grit size of 60 to those prepared using polish grit. Furthermore, in the same range, the mountain peak of the surface microscopic topography was reduced significantly, and regular ups and downs were formed at a micro level. Fig. 8 shows the average surface roughness of all types of samples. Clearly, the surface roughness of samples decreases with the increase of the grit size of sandpaper.

In the material bonding system, the main factors affecting the mechanical interlocking, when the adhesive sufficiently wets the substrates, are roughness, porosity, and irregularity of the bonding surface [12,33], where the surface porosity and irregularity can be understood as the density of summits and the morphology of crest, respectively. At the same time, excessive surface roughness can affect the diffusion of the adhesive, which in turn influences the bonding effect. Based on the above mentioned information and considering the single lap joint as an example, the bonding diagrams of different types of specimens in group B are shown in Fig. 9. Fig. 9(a) shows that for the specimens treated using sandpaper with grit size of 60; although the surface roughness of the specimen is the largest, the mechanical interlocking effect is relatively poor. The reasons can be summarized as follows: (a) on a macro-scale, a large amount of fibers on the substrate surface were cut off by abrasive grains; therefore, the integrity of many fibers on the surface was destroyed seriously as shown in Fig. 6(a). (b) On a micro-scale, the fluctuation of the bonding surface was dramatic and inhomogeneous as shown in Fig. 7(a), consequently, uneven distribution of the adhesive occurred. (c) The excessive surface roughness prevented the fluidity of the adhesive, the adhesive did not penetrate well into the rough surface, and gas molecules were trapped in the valleys. As a result, many adhesive non-permeability zones and an alternation of solid–liquid and gas–liquid interfaces were formed as shown in Fig. 9 (blue part). In contrast, for the specimens abraded using sandpapers with grit sizes of 220, 400, 800, and polish finish (Fig. 9(b)–(e)), the surface of the samples was relatively more integrated, and the surface microscopic contour was homogeneous. Therefore, the surface roughness is the main factor affecting the mechanical interlocking. Consequently, in terms of mechanical interlocking action, the tensile strength of the samples should be decreased gradually from the grit size of 220 to polish grit.

3.2.2. Contact angle and surface energy

Figs. 10 and 11 show the average contact angle and surface energy of the bonding surfaces for various specimens, respectively. Clearly, the surface contact angles of the samples tend to decrease first and then increase gradually with the increase of the grit sizes for both the single lap joint and scarf adhesive joint. In other words, the surface wettability of the specimens was affected by the surface roughness. In contrast, the

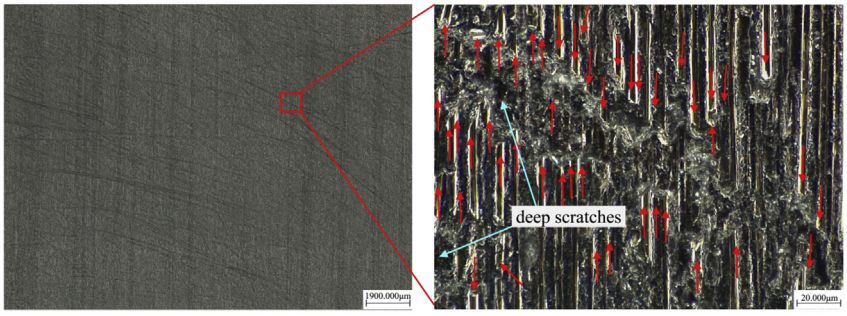

(a)

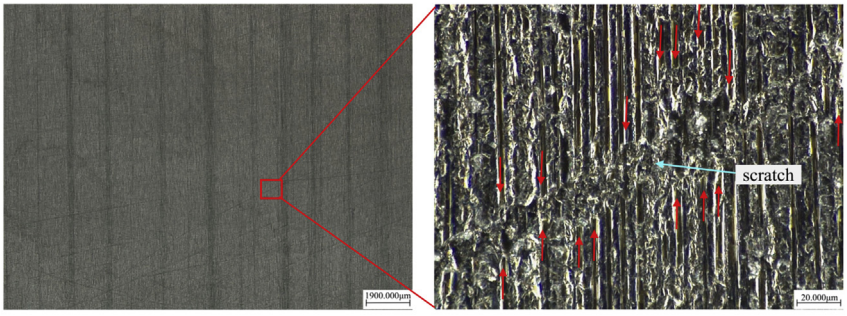

(b)

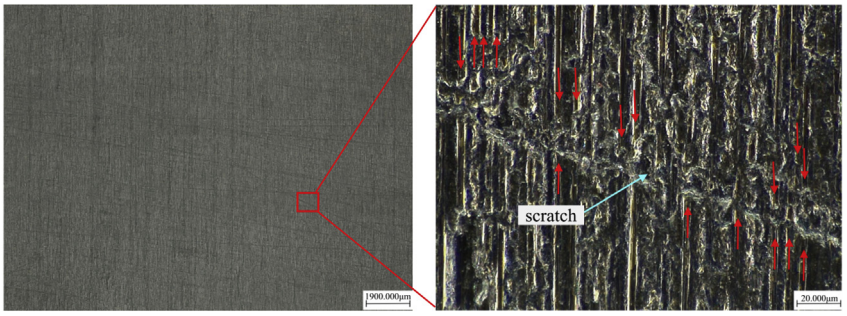

(c)

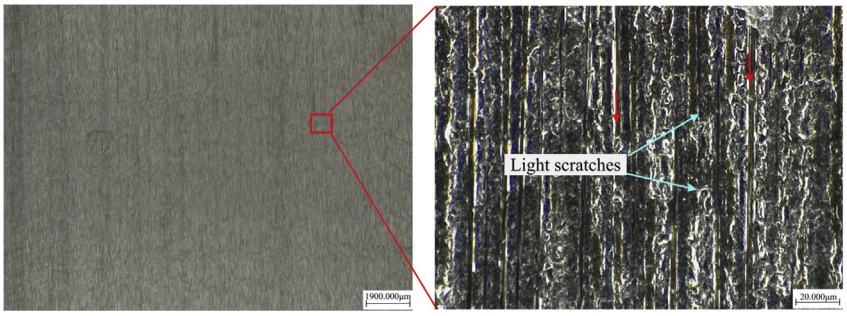

(d)

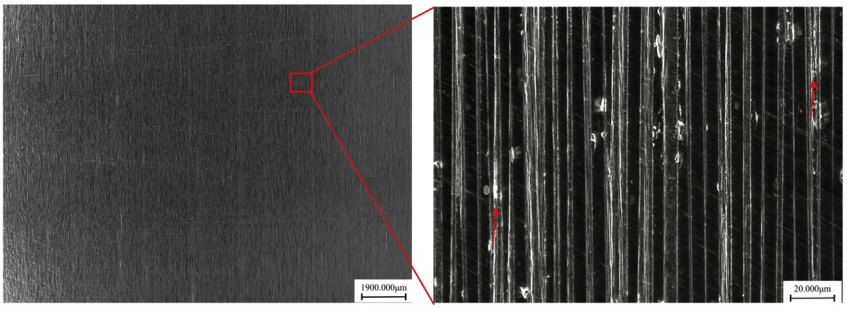

(e)

(caption on next page)

Fig. 6. The macroscopic topography (left) and local magnification (right) of the bonding surface prepared with (a) 60, (b) 220, (c) 400, (d) 800 grit sizes of sandpapers and (e) polish of single lap joint (The red represents the broken fiber at the scratch). (For interpretation of the references to colour in this figure legend, the reader is referred to the Web version of this article.)

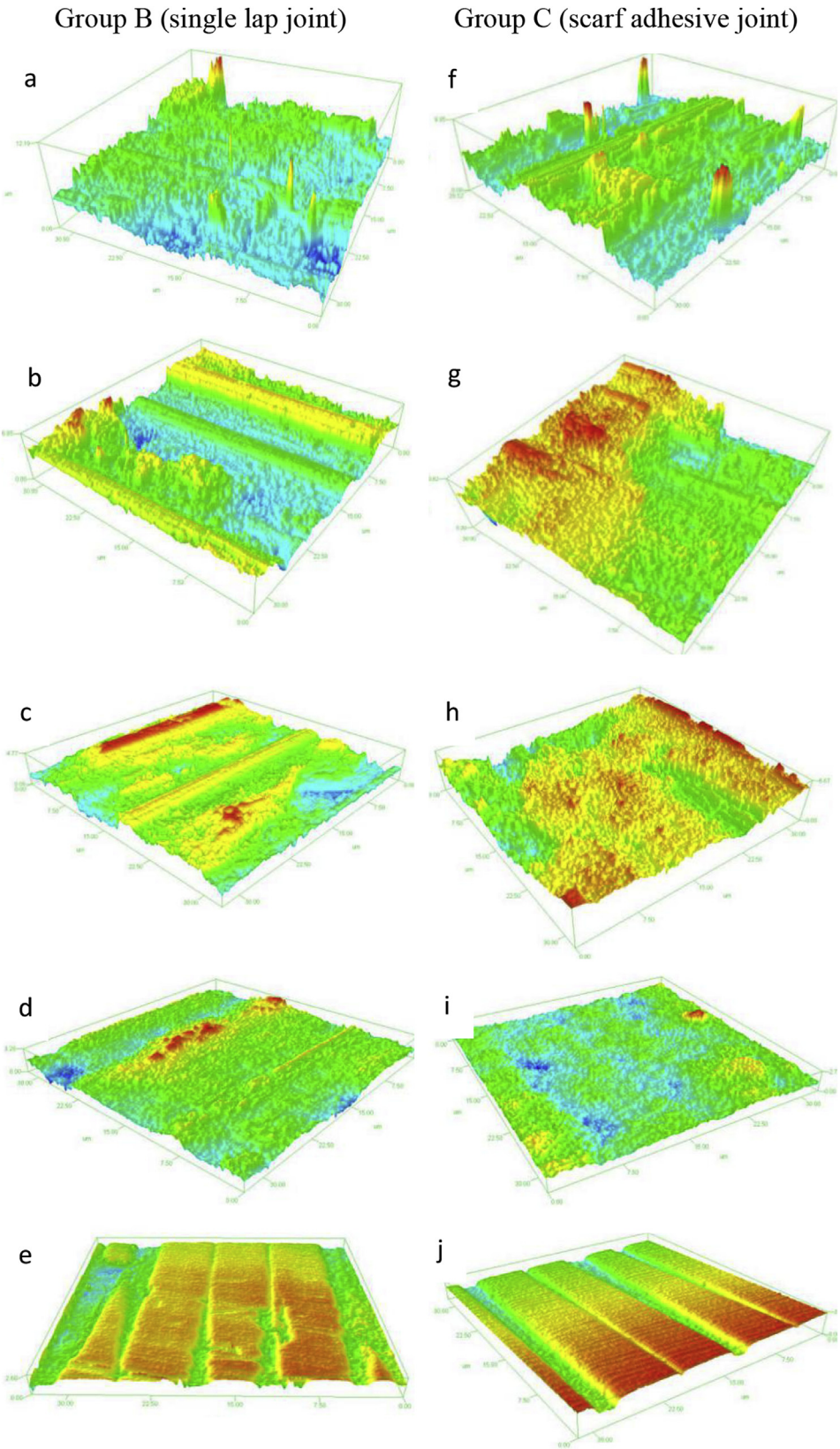

Fig. 7. The 3D microscopic topography of the bonding surface prepared with (a、f) 60, (b、g) 220, (c、h) 400, (d、i) 800 grit sizes of sandpapers and (e、j) polish.

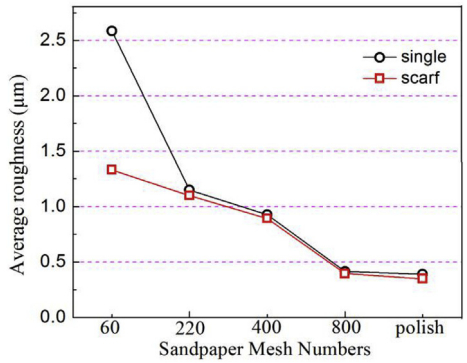

Fig. 8. The average surface roughness of the single lap joint and scarf adhesive joint.

surface energy appears to represent the trend opposite to that of the surface contact angle. Furthermore, the polar and dispersion components of the surface energy of various specimens differ significantly from each other, and the polar components are generally smaller than dispersion components. The theory of adhesive adsorption holds that the greater the surface free energy of the specimens, the stronger the bonding force with the external matter, and consequently, the better the bonding effect. Therefore, in terms of the theory of adhesive adsorption, the tensile strength of the samples should increase first and then decrease gradually from the grit size of 220 to polish grit.

The above mentioned analysis combined with Fig. 5(b) and (c) indicates that the changing trend of shear strength for the single lap specimens is consistent with the result of mechanical interlocking effect that the shear strength decreases slightly with the increase in the grit size of the sandpaper from 220 grit to polish finish. The specimens treated using sandpaper with grit size of 220 were compared with those sanded with 800 grit sandpaper. First, their surface roughness was 1.15 and 0.41 μm, respectively. Therefore, the mechanical interlocking worked better when grit size was 220. Second, the surface energy of specimens sanded with 220 and 800 grits sandpapers was 36.4622 and 36.31 mJ/m^2, respectively. Furthermore, the shear strength exhibits a significant relationship with the polar component of the surface energy, and the shear strength of the samples should become better with the increase in the polar component [10,24]. Moreover, the samples sanded with 800 grit size sandpaper exhibits a larger polar component than that with 220 grit sandpaper. Therefore, the samples sanded with grit size 800 possessed better adsorption effect. According to Fig. 5(b); however, the shear strength of the sample treated using sandpaper with grit size 220 is greater than that with 800, thus it can be concluded that the mechanical interlocking effect on the bond strength of the single lap joints is greater than adsorption effect. The same conclusion could be drawn when the grit sizes 220 and 400 were compared.

For the scarf adhesive joint, the samples ground using the sandpaper with the grit size of 60 appeared to have the worst bonding strength which was similar to that of single lap joint. This was due to the fact that many surface fibers of the substrates were broken by abrasive grains. Comparative analysis of the specimens sanded by grit sizes 220 and 400 indicates that the surface roughness is 1.10 and 0.89 μm respectively; therefore, the mechanical interlocking works better for grit size of 220. Furthermore, the surface energy is 31.36 and 36.9 mJ/m^2, respectively, which indicates that the samples sanded with grit size 400 possessed better adsorption effect. Fig. 5(c) demonstrates that the tensile strength of the specimens sanded by grit size 400 is greater than that by 220, and the changing trend of the tensile strength for scarf adhesive joint is consistent with the adsorption analysis results. Therefore, for the scarf adhesive joint, the effect of adsorption on the bonding strength was greater than the mechanical interlocking, which was different from the single lap joints. This is due to the fact that the effect of mechanical interlocking on the bonding strength depends on the direction of the applied force [12]. Fig. 12 shows the force of the adhesive layer under tensile load for the scarf adhesive joint. The mechanical interlocking enhances only the shear stress along the slope direction and has little effect on the peeling stress, which is perpendicular to the slope. Subsequently, the total mechanical interlocking effect on the scarf adhesive joint is not as obvious as on the single lap joints.

3.3. Analysis of failure morphology

Fig. 13 shows the typical failure morphology of various specimens. For the single lap joints, almost all types of specimens were characterized by cohesion failure of adhesive except for the samples corresponding to the grit size 60. Fig. 13(a) shows that the specimens sanded with grit size 60 exhibits an obvious mixed failure mode including cohesion and fiber tearing. This phenomenon could be attributed to the fact that the integrity of the surface fiber of the specimens sanded by grit size 60 was destroyed, and the fibers cut off by abrasive grains were easily torn away from the substrate during the tensile load, which was consistent with the results of the previous studies that the destruction of surface fiber resulted in the decrease of substrate strength, and further led to the failure mode of fiber tearing [34,35].

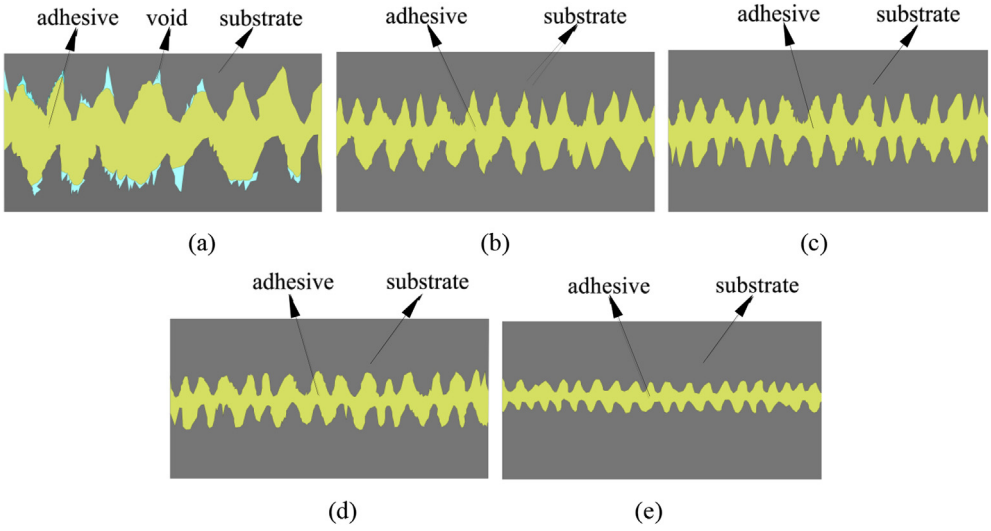

Fig. 9. The bonding diagram of different types of substrates prepared with (a) 60, (b) 220, (c) 400, (d) 800 grit sizes of sandpapers and (e) polish of single lap joint.

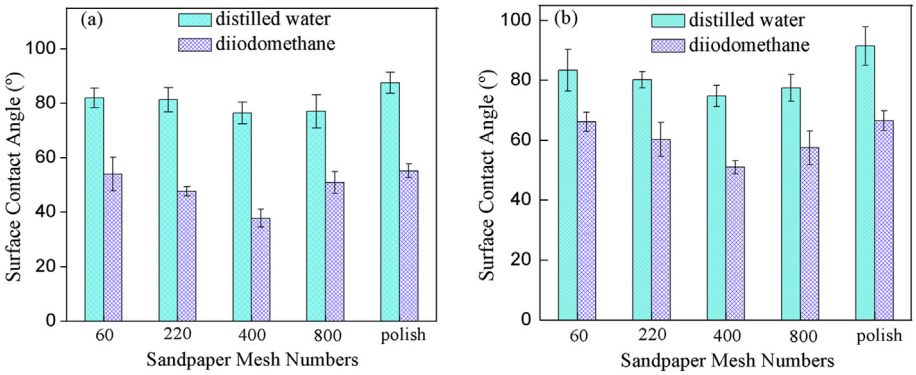

Fig. 10. The average surface contact angle of the bonding surfaces for (a) the single lap joint and (b) scarf adhesive joint.

For the parts of cohesion failure of specimens sanded using sandpaper with grit size 60, the failed adhesive appeared as scaly colloidal layer distributed along the grinding traces as shown in local magnification of Fig. 13(a). Excessive surface roughness prevented the fluidity of adhesive and limited the flow direction to a certain extent when the samples were bonded. Therefore, the adhesive aggregated at the grinding traces and formed many resin-rich regions. For the specimens abraded using sandpapers with grit sizes of 220, 400, 800, and polish grit, the failure morphology of the adhesive layer exhibited a gradually uniform and close grain as shown in the local magnification of various specimens presented in Fig. 13(b–e). This could be attributed to the fact that the bonding surface became gradually smooth, the scratch on the bonding surface appeared to be shallower, and the adhesive layer distribution was homogeneous consequently. Noteworthy, for the specimens sanded by grit size 800 and polish processing, pores occurred in the adhesive layer as shown in Fig. 13(d) and (e). This phenomenon could be attributed to the fact that the substrate surface was too smooth that there was no way for gas molecules to escape, consequently the gas molecules were trapped in adhesive layer when the specimens were bonded, which was different from the roughness surface that the air in the grooves or gaps would be well discharged [21].

For the scarf adhesive joints, Fig. 13(f–g) show that specimens exhibit a mixed failure mode of cohesion and fiber tearing, which was different from the behavior of single-lap joints. Previous studies indicated that the failure mode of the adhesive joint appeared to be related to material strength of adhesive. In the case of lower material strength of adhesive, the cohesion failure was critical. On the other hand, the fiber tearing was critical in the case of higher material strength of adhesive [35]. For the bonding area with 0° fiber, the material strength of the substrate was greater than that of the adhesive, and on the other hand, the material strength of adhesive was greater for the bonding area of 90°. Therefore, for the scarf adhesive joints, the

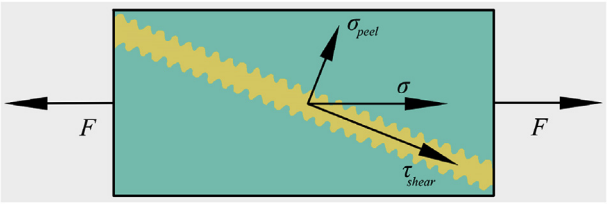

Fig. 12. The force diagram of the scarf adhesive joint under the tensile load.

fiber tearing mainly occurred on the 90° fiber, while the bonding area of 0° fiber mainly failed due to the cohesion failure of the adhesive as shown in Fig. 13(f–g). This result was in accordance with the previous studies that the fiber stacking angle of the bonded surface would directly affect the failure mode of the adhesive joints [36]. Owing to this failure mode, the influence of surface characteristics on the bonding strength could not be reflected very well. Half of the area on the bonding surface failed with the substrate, which was related to the nature of material but had little to do with surface characteristics [37,38]. Therefore, the difference of bonding strength between each group of scarf adhesive joints was not as significant as in case of the single lap joints, which is consistent with the results of the variance analysis. Above all, it can be concluded that the influence of surface treatment on the bonding strength is related to the failure mode and the joint types.

4. Conclusion

The effects of roughness of the sandpaper and the direction of grinding on the tensile strength of the adhesive joints were experimentally studied. The results are summarized as follows:

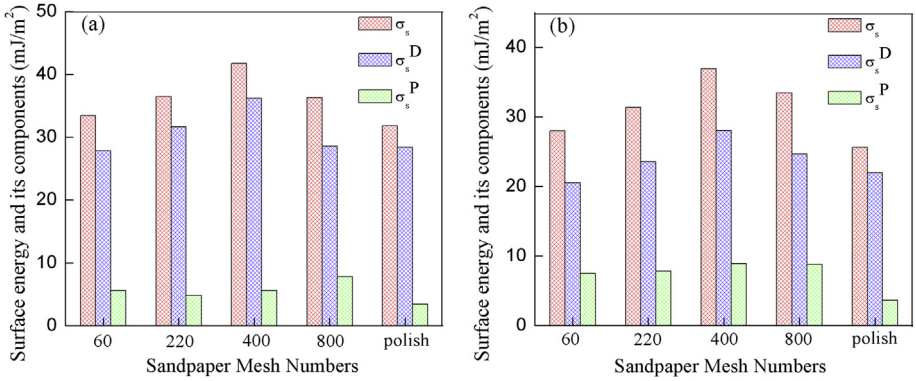

Fig. 11. The surface energy of the bonding surfaces for (a) the single lap joint and (b) scarf adhesive joint. (σ_s represents the total surface energy, and σ_s^D and σ_s^p correspond to the dispersive and polar fractions, respectively.)

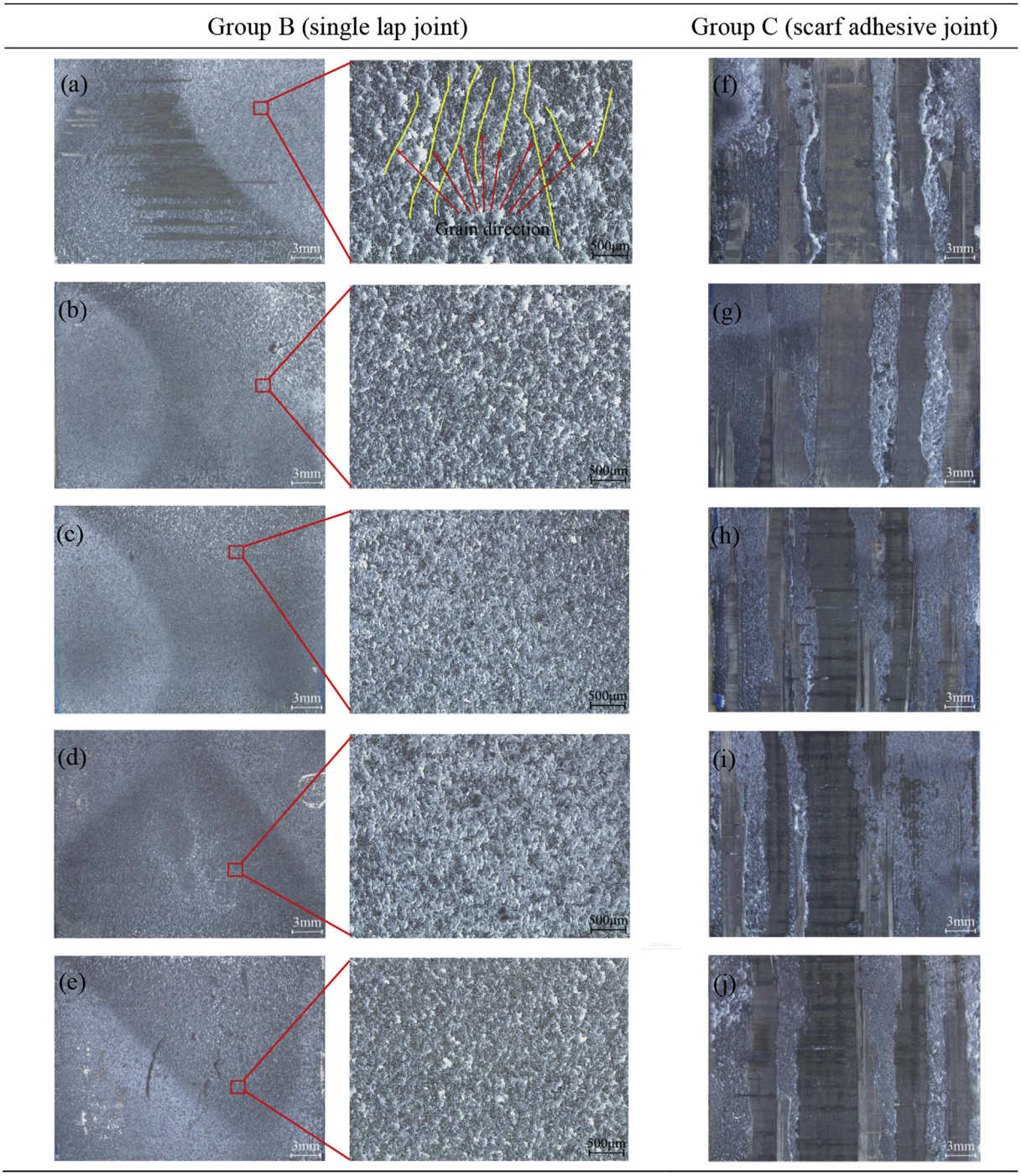

Fig. 13. The typical failure mode of various specimens prepared with (a、f) 60, (b、g) 220, (c、h) 400, (d、i) 800 grit sizes of sandpapers and (e、j) polish.

1. The sanding direction significantly affected the tensile strength of the joints. The best bonding performance was obtained when the surface was abraded in the random direction. Moreover, the shear strength was 9.91 and 9.16% higher than that of unidirectional grinding (parallel to the fiber direction and perpendicular to the fiber direction), respectively.
2. For both the single lap joints and scarf adhesive joints, the tensile strength of the specimens first increased and then decreased slightly with the increase in the grit size of sandpaper. This trend of tensile strength could not be explained simply by the increased roughness characteristics which is related to the mechanical interlocking. Furthermore, it was associated with the surface energy, which is related to the effect of adsorption. For the single lap joints, the effect of mechanical interlocking on the bonding strength was more significant. In contrast, for the scarf adhesive joints, the effect of adsorption on the bond strength worked well.
3. The influence of surface treatment on bonding strength was related to the failure mode and the joint types. For the single lap joints, the failure mode was characterized by cohesion failure of adhesive layer, and the surface properties of the substrate significantly influenced the tensile strength. However, for the scarf adhesive joints, the main failure modes of the samples were the tearing at the 90° fiber and the cohesion failure of adhesive layer at the 0° fiber. This phenomenon resulted that the influence of the surface characterizations on the tensile strength was not as significant as the single lap joints.

4. For the single lap joints, optimum shear strength was obtained when samples were abraded using sandpaper with grit size of 220, and the shear strength increased by 17.62 and 22.31%, respectively, compared to the grit sizes of 60 and polish processing. For the scarf adhesive joints, the maximum tensile strength was achieved when samples were abraded with 400 grit size, and the tensile strength increased by 11 and 8.9%, respectively, compared to the grit sizes of 60 and polish processing. This phenomenon indicated that the relationship between the tensile strength of joint and the surface roughness is not simply proportional or inverse, but has an optimum value.

Acknowledgment

The authors gratefully acknowledge the financial support from the National Natural Science Foundation of China (Grant No. 11372220).

References

[1] Yao MX, Zhu DJ, Yao YM, Zhang HA, Mobasher B. Experimental study on basalt FRP/steel single-lap joints under different loading rates and temperatures. Compos Struct 2016;145:68–79.
[2] Fawzia S. Evaluation of shear stress and slip relationship of composite lap joints. Compos Struct 2013;100(5):548–53.
[3] Araújo HAM, Machado JJM, Marques EAS, da Silva LFM. Dynamic behaviour of composite adhesive joints for the automotive industry. Compos Struct 2017;171:549–61.
[4] Caminero MA, Pavlopoulou S, Lopez-Pedrosa M, Nicolaisson BG, Pinna C, Soutis C. Analysis of adhesively bonded repairs in composites: damage detection and prognosis. Compos Struct 2013;95:500–17.
[5] Cheng P, Gong XJ, Hearn D, Aivazzadeh S. Tensile behaviour of patch-repaired CFRP laminates. Compos Struct 2011;93:582–9.
[6] Kim MK, Elder DJ, Wang CH, Feih S. Interaction of laminate damage andadhesive disbonding in composite scarf joints subjected to combined in-planeloading and impact. Compos Struct 2012;94:945–53.
[7] Andrew JJ, Arumugam V, Santulli C. Effect of post-cure temperature and different reinforcements in adhesive bonded repair for damaged glass/epoxy composites under multiple quasi-static indentation loading. Compos Struct 2016;143:63–74.
[8] Machado JJM, Gamarra PMR, Marques EAS, da Silva LFM. Improvement in impact strength of composite joints for the automotive industry. Compos B Eng 2017;138:243–55.
[9] Machado JJM, Marques EAS, Campilho RDSG, da Silva LFM. Mode II fracture toughness of CFRP as a function of temperature and strain rate. Compos B Eng 2017;114:311–8.
[10] Gude MR, Prolongo SG, Ureña A. Adhesive bonding of carbon fibre/epoxy laminates: correlation between surface and mechanical properties. Surf Coating Technol 2012;207(9):602–7.
[11] Rhee KY, Lee SG, Choi NS, Park SJ. Treatment of CFRP by IAR method and its effect on the fracture behavior of adhesive bonded CFRP/aluminum composites. Mater Sci Eng, A 2003;357(1–2):270–6.
[12] Baldan A. Adhesion phenomena in bonded joints. Int J Adhesion Adhes 2012;38(4):95–116.
[13] Islam MS, Tong L, Falzon PJ. Influence of metal surface preparation on its surface profile, contact angle, surface energy and adhesion with glass fibre prepreg. Int J Adhesion Adhes 2014;51:32–41.
[14] Xu Z, Chen L, Huang Y, Li J, Wu X, Li X, Jiao Y. Wettability of carbon fibers modified by acrylic acid and interface properties of carbon fiber/epoxy. Eur Polym J 2008;44(2):494–503.
[15] Baburaj EG, Starikov D, Evans J, Shafeev GA, Bensaoula A. Enhancement of adhesive joint strength by laser surface modification. Int J Adhesion Adhes 2007;27(4):268–76.
[16] Coulon JF, Tournerie N, Maillard H. Adhesion enhancement of Al coatings on carbon/epoxy composite surfaces by atmospheric plasma. Appl Surf Sci 2013;283(14):843–50.
[17] Osouli-Bostanabad K, Tutunchi A, Eskandarzade M. The influence of pre-bond surface treatment over the reliability of steel epoxy/glass composites bonded joints. Int J Adhesion Adhes 2017;75:145–54.
[18] Rotel M, Zahavi J, Tamir S, Buchman A, Dodiuk H. Pre-bonding technology based on excimer laser surface treatment. Appl Surf Sci 2000;154(154):610–6.
[19] Shaker M, Salahinejad E. A combined criterion of surface free energy and roughness to predict the wettability of non-ideal low-energy surfaces. Prog Org Coating 2018;119:123–6.
[20] Lim JD, Yeow SYS, Rhee MWD, Kam CL, Chee CW. Surface roughness effect on copper–alumina adhesion. Microelectron Reliab 2013;53(9–11):1548–52.
[21] Zhan X, Li Y, Gao C, Wang H, Yang Y. Effect of infrared laser surface treatment on the microstructure and properties of adhesively CFRP bonded joints. Optic Laser Technol 2018;106:398–409.
[22] Osouli-Bostanabad K, Tutunchi A, Eskandarzade M. The influence of pre-bond surface treatment over the reliability of steel epoxy/glass composites bonded joints. Int J Adhesion Adhes 2017;75:145–54.
[23] Rotel M, Zahavi J, Tamir S, Buchman A, Dodiuk H. Pre-bonding technology based on excimer laser surface treatment. Appl Surf Sci 2000;154(154):610–6.
[24] Encinas N, Oakley BR, Belcher MA, Blohowiak KY, Dillingham RG, Abenojar J, et al. Surface modification of aircraft used composites for adhesive bonding. Int J Adhesion Adhes 2014;50(4):157–63.
[25] Reitz V, Meinhard D, Ruck S, Riegel H, Knoblauch V. A comparison of IR- and UV-laser pretreatment to increase the bonding strength of adhesively joined Aluminum/CFRP components. Compos A Appl Sci Manuf 2017;96:18–27.
[26] Palmieri FL, Belcher MA, Wohl CJ, Blohowiak KY, Connel JW. Laser ablation surface preparation for adhesive bonding of carbon fiber reinforced epoxy composites. Int J Adhesion Adhes 2016;68:95–101.
[27] Junior SAR, Ferracane JL, Della Bona A. Influence of surface treatments on the bond strength of repaired resin composite restorative materials. Dent Mater 2009;25(4):442–51.
[28] Wetzel M, Holtmannspötter J, Gudladt HJ, Czarnecki JV. Sensitivity of double cantilever beam test to surface contamination and surface pretreatment. Int J Adhesion Adhes 2013;46:114–21.
[29] Rhee KY, Yang JH. A study on the peel and shear strength of aluminum/CFRP composites surface-treated by plasma and ion assisted reaction method. Compos Sci Technol 2003;63(1):33–40.
[30] Boutar Y, Naïmi S, Mezlini S, Ali MB. Effect of surface treatment on the shear strength of aluminium adhesive single-lap joints for automotive applications. Int J Adhesion Adhes 2016;67:38–43.
[31] Rudawska A, Jacniacka E. Analysis for determining surface free energy uncertainty by the Owen–Wendt method. Int J Adhesion Adhes 2009;29(4):451–7.
[32] Astm D. Standard test method for tensile properties of polymer matrix composite materials. 2008.
[33] Yang S, Gu L, Gibson RF. Nondestructive detection of weak joints in adhesively bonded composite structures. Compos Struct 2001;51(1):63–71.
[34] Sun C, Min J, Lin J, Wan H, Yang S, Wang S. The effect of laser ablation treatment on the chemistry, morphology and bonding strength of CFRP joints. Int J Adhesion Adhes 2018;84:325–34.
[35] Kim KS, Yoo JS, Yi YM, Kim CG. Failure mode and strength of uni-directional composite single lap bonded joints with different bonding methods. Compos Struct 2006;72(4):477–85.
[36] Demiral M, Kadioglu F. Failure behaviour of the adhesive layer and angle ply composite adherends in single lap joints: a numerical study. Int J Adhesion Adhes 2018;87:181–90.
[37] Li J, Yan Y, Zhang T, Liang Z. Experimental study of adhesively bonded CFRP joints subjected to tensile loads. Int J Adhesion Adhes 2015;57:95–104.
[38] Banea MD, da Silva LFM, Carbas R, Campilho RDSG. Effect of material on the mechanical behaviour of adhesive joints for the automotive industry. J Adhes Sci Technol 2017;31(6). 14.